JOURNAL OF SPACECRAFT AND ROCKETS
Vol. 35, No. 4, July–August 1998

Dynamic Oxidation Performance of NARloy-Z with Cu-30 Volume Percent Cr Coating

T. A. Wallace* and R. K. Clark†
NASA Langley Research Center, Hampton, Virginia 23681
and
K. T. Chiang‡
The Boeing Company, Canoga Park, California 91303

The copper alloy NARloy-Z (Cu-3Ag-0.5Zr wt%) has good potential for high heat flux structural applications in hypersonic vehicles because of its high thermal conductivity and high-temperature strength. However, it is subject to severe oxidation at temperatures where it might be used. A Cu-30 vol% Cr protective coating produced by low-temperature arc vapor deposition was evaluated under dynamic oxidation in an electric arc-heated wind tunnel. The emittance of the coating is greater than the emittance of the alloy, and the recombination efficiency of the coating is typical of values encountered with metal alloys and metallic oxides. The coating protects the alloy under dynamic oxidation conditions, with specimens gaining less than 1 mg/cm^2 over a 10-h exposure period. Protection of the alloy from oxidation results from a continuous layer of Cr_2O_3 that it is partially shielded from the hostile dynamic oxidation/atomic oxygen environment by a layer of CuO.

Nomenclature

c_{ins} = insulator heat capacity, J/kg · K
c_p = specimen heat capacity, J/kg · K
$e_b(\lambda, T)$ = blackbody emissive power at T and λ, W/m^2
k = specimen thermal conductivity, W/m · K
k_{ins} = insulator thermal conductivity, W/m · K
k_w = catalytic reaction rate constant, m/s
l = specimen thickness, m
l_{ins} = insulator thickness, m
M_A = average molecular weight of dissociated species, kg/mole
q_{absorp} = heat absorption by specimen, W/m^2
q_{aero} = aerothermal heat transfer, W/m^2
q_C = heat transfer to specimen by convection, W/m^2
q_{cond} = heat loss from specimen by conduction, W/m^2
q_D = heat transfer to specimen by diffusion, W/m^2
q_{rad} = heat loss by specimen through radiation, W/m^2
R_u = universal gas constant, j/mole · K
S = boundary-layer diffusion rate, m/s
T = specimen temperature, K
T_b = temperature at insulator back surface, K
T_0 = initial temperature of specimen, K
β = test stream velocity gradient, s^{-1}
γ = recombination efficiency of specimen surface
$\partial T/\partial t$ = temperature rise rate of specimen, K/s
ε_{TH} = total hemispherical radiative emittance
ε_{TN} = total normal radiative emittance
$\varepsilon(\lambda, T)$ = near-normal spectral emittance at λ and T
λ = wavelength, m
μ_{se} = freestream test gas viscosity, Pa/s
μ_w = test gas viscosity at specimen wall, Pa/s
ρ = specimen density, kg/m^3
ρ_{se} = freestream test gas density, kg/m^3
ρ_w = test gas density at specimen wall, kg/m^3
σ = Stephan–Boltzman constant, W/m^2 · K^4
ϕ = recombination factor

Received July 29, 1997; revision received Dec. 20, 1997; accepted for publication Dec. 23, 1997.

*Materials Research Engineer, Materials Division.
†Retired.
‡Member of the Technical Staff, Rocketdyne Propulsion and Power Systems, Boeing North American, Inc., 6633 Canoga Avenue. Member AIAA.

Introduction

COPPER-BASED alloys are candidate materials for high heat flux structural applications in hypersonic vehicles because of their high thermal conductivity and high-temperature strength. A major limitation to the use of copper-based materials is their rapid oxidation at elevated temperatures. Protective coatings that shield these materials from oxidation must be employed to enable their use at temperatures to 920 K. Additionally, coatings with favorable thermal control characteristics such as a high emittance and low-recombination efficiency surface may further enhance their performance in hypersonic vehicle applications.

One approach to a protective coating for copper-based alloys utilizes chromia scales like those formed on M–Cr alloys (where M is Fe, Ni, or Co), which impart oxidation resistance when formed on the alloy. One practical requirement of such coatings is that the chromium concentration at the surface must be high enough to form a continuous Cr_2O_3 scale, which must be stable in the service environment.

References 1 and 2 showed that Cu-30 vol% Cr coatings produced by low-temperature arc vapor deposition (LTAVD) form a protective Cr_2O_3 scale on Cu-Nb alloy in static air in the temperature range 773–973 K. However, Ref. 3 showed that oxidative vaporization of Cr_2O_3 in oxygen is enhanced by about 10^9 at 825 K in the presence of 2.5% oxygen atoms by enhancing the reaction $Cr_2O_{3(s)} + 3O_{(g)} \rightarrow 2CrO_{3(g)}$. Also when TD-Ni-20Cr, a thoria dispersion strengthened alloy that has good oxidation resistance in static environments due to the formation of a protective Cr_2O_3 layer, is exposed to high-speed flow containing atomic oxygen, the Cr_2O_3 is rapidly lost.[4] Because of these prior results, there is concern that the Cu-30 vol% Cr coating will not protect copper-based alloys employed in hypersonic vehicle applications where atomic oxygen may be present.

This study was initiated to evaluate the performance of the NARloy-Z with an LTAVD Cu-30 vol% Cr coating in hypersonic environments using the hypersonic materials environmental test system (HYMETS) at the NASA Langley Research Center. All tests were performed at the anticipated upper use temperature of 920 K, and this paper presents the oxidation weight change, surface emittance, and surface recombination efficiency results. The results are contrasted with data from static oxidation tests and dynamic oxidation tests of uncoated NARloy-Z. The morphology and chemical composition of the surface of coated specimens were characterized

before and after oxidation exposure by light microscopy, scanning electron microscopy (SEM) with energy dispersive x-ray spectroscopy (EDS), and x-ray diffraction (XRD) using a copper radiation tube. Some specimens were cross sectioned and examined by SEM with EDS and light microscopy.

Material Specimens

Specimens were 2.5-cm-diam disks cut from 0.51-mm-thick NARloy-Z sheet. The nominal weight percent composition of NARloy-Z is Cu-3Ag-0.5Zr. Specimens were coated on all surfaces with a 50–75-μm-thick Cu-30 vol% Cr coating. Specimens were supplied for testing in the as-coated condition and in a preoxidized condition that involved a postcoat static oxidation treatment in laboratory air at 920 K for 22 h.

The coating was applied by codeposition of Cu and Cr using the LTAVD technique described in Ref. 2. The LTAVD process[5] is a patented variation of the cathodic arc plasma deposition process.[6,7] It utilizes a cylindrically shaped cathode material for evaporation. During coating, one or more arc spots are generated on the cathode and traverse along the cathode surface to cause flash evaporation of the cathode material. The evaporants consist of a large flux of high-energy ions along with microdroplets and some metal vapors. The microdroplets are metal particles that leave the cathode in a molten state because of localized melting by the arc. With the ability to deposit tightly adherent metallic coatings even at ambient temperatures, this technique has previously been used for metallizing plastics to address electrical, optical, thermal, corrosion/oxidation, mechanical, and decorative requirements.[8,9]

Experiment

Coated specimens of NARloy-Z were tested at 920 K under dynamic oxidation conditions in an as-coated state and in a preoxidized state, where the coated specimen was given a static oxidation treatment in laboratory air at 920 K for 22 h. In addition to tests of coated specimens, uncoated specimens of NARloy-Z and unalloyed chromium were tested at 920 K under static oxidation conditions in a laboratory furnace and under dynamic oxidation conditions.

The dynamic oxidation tests were performed at a temperature of 920 K for times to 10 h in the HYMETS[10] at the NASA Langley Research Center. The HYMETS is a 100-kW, constrictor-arc-heated wind tunnel that uses air plus nitrogen and oxygen in ratios equivalent to air to produce the test environment. The test gas is a mixture of air plus nitrogen and oxygen in ratios equivalent to air. High-purity nitrogen is introduced at the cathode, and air and high-purity oxygen are introduced in the plenum upstream of the supersonic nozzle. A schematic diagram of the facility is shown in Fig. 1.

Specimens are mounted on stagnation model adapters attached to pneumatically actuated struts so that flow of gases is normal to the specimen surface. The temperature of a specimen is monitored during exposure by a thermocouple attached to its back surface or by a radiation pyrometer focused on its front surface. A water-cooled probe that measures the rate of catalytic cold-wall heat transfer to the specimen and the specimen surface pressure is mounted on a different strut.

The test conditions attainable in the HYMETS are not equivalent to the environment associated with high-heat flux structural applications of hypersonic vehicles; however, the environment does contain high-speed flowing gas with atomic and molecular oxygen, which is

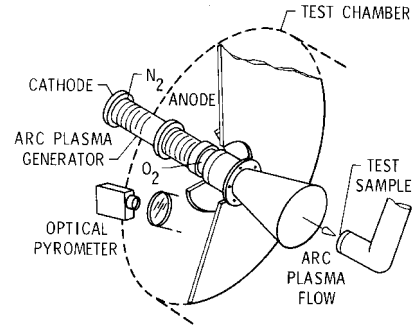

Fig. 1 Diagram of NASA Langley Research Center HYMETS.

Table 1 Range of operating conditions for HYMETS facility

Parameter	Range
Mach number	3.5–4.4
Wall pressure, Pa	525–850
Stream enthalpy, MJ/kg	3.5–10.0
Catalytic cold-wall heating rate, kW/m^2	60–425
Equilibrium dissociation, %	
Oxygen	0–100
Nitrogen	$\leq$5

of critical concern to using chromium-containing materials in hypersonic vehicle applications. The ranges of operating conditions of the HYMETS facility are shown in Table 1. Chemical equilibrium calculations for the operating conditions of the present study indicate that oxygen in the test stream was almost fully dissociated (>95%) and the nitrogen was only slightly dissociated (<5%) (Ref. 11).

Tests consisted of cyclic exposure of specimens for half-hour periods at 920 K for an accumulated exposure of up to 10 h. The specimens were cooled to room temperature after each heating period. The specimen temperature was maintained at 920 K by adjusting the power input to the test facility. The nominal stream test conditions for the tests were 3.7 Mach number, 530-Pa wall pressure, and 3.6-MJ/kg stream enthalpy.

Coating Analysis

The change in weight of specimens during exposure was determined periodically by removing them from the HYMETS and weighing them on an analytical balance. The morphology and chemical composition of the surface of specimens were characterized, before and after exposure to the HYMETS environment, by light microscopy, SEM with EDS, and XRD using a copper radiation tube. Some specimens were cross sectioned and examined by SEM with EDS and light microscopy.

Room-temperature spectral near-normal reflectance measurements were made over the wavelength range from 1.5 to 25 μm using a Gier Dunkle Model HCDR 3 heated-cavity reflectometer.[12] Spectral emittance is calculated from the reflectance using the relationships that absorptance equals unity minus reflectance and (from Kirchhoff's law) spectral emittance equals spectral absorptance. Total emittance is calculated from spectral emittance using the following equation[13]:

$$\varepsilon_{TN} = \frac{\sum \varepsilon(\lambda) e_b(\lambda, T)\Delta\lambda}{\sum e_b(\lambda, T)\Delta\lambda} \tag{1}$$

Heat transfer analyses require total hemispherical emittance data. Total hemispherical emittance data are obtained from the ratio[14]

$$\varepsilon_{TH}/\varepsilon_{TN} = 0.975 \tag{2}$$

Recombination efficiency is the probability that a gaseous atom striking the surface will combine with a like atom to form a molecule. It can be calculated from an energy balance at the surface. The aerothermal heating to a specimen in hypersonic flow is the sum of the convection heating and the catalytic heating:

$$q_{aero} = q_C + q_D\phi \tag{3}$$

where q_C and q_D are determined from Goulard's solution for the stagnation point laminar heat transfer equation for a surface with a finite recombination efficiency.[15,16] The recombination factor accounts for the fraction of heat transfer resulting from recombining of atomic species at the surface. The recombination factor is related to recombination efficiency of the surface through the relationships

$$\phi = \frac{1}{1 - (S/k_w)} \tag{4}$$

$$S = 0.763\left[\frac{\mu_w \rho_w}{\mu_{se}\rho_{se}}\right]^{0.1}\sqrt{\beta\mu_{se}\rho_{se}} \tag{5}$$

$$k_w = \gamma\sqrt{R_u T/2\pi M_A} \tag{6}$$

The aerothermal heating to the specimen is balanced by heat absorption by the specimen, heat reradiated by the specimen surface, and heat lost by conduction to the specimen holder:

$$q_{\text{aero}} = q_{\text{absorp}} + q_{\text{rad}} + q_{\text{cond}} \tag{7}$$

where

$$q_{\text{absorp}} = \rho c_p l \frac{\partial T}{\partial t} \tag{8}$$

$$q_{\text{rad}} = \varepsilon_{\text{TH}} \sigma T^4 \tag{9}$$

$$q_{\text{cond}} = 2\sqrt{\frac{\rho_{\text{ins}} c_{\text{ins}} k_{\text{ins}}}{\pi}(T_s - T_0)\frac{\partial T}{\partial t}} \tag{10}$$

for transient heating and

$$q_{\text{cond}} = \frac{k_{\text{ins}}(T - T_b)}{l_{\text{ins}}} \tag{11}$$

for thermal equilibrium conditions.

The calculated heating rate and the measured fully catalytic heating rate for the same test conditions are used with Goulard's solution to determine the recombination efficiency of the specimen surface at the test temperature.[16] Principle assumptions invoked in obtaining this solution include the following: The stagnation laminar boundary-layer solution is valid, expansion of the gases in the nozzle is isentropic, and chemistry of the gases is frozen in the boundary layer. The two steps in the calculation process are as follows: 1) The measured fully catalytic heating rate is used with Goulard's solution[16] to determine the enthalpy of the test environment, and 2) the calculated heating rate [Eq. (7)] is used with Goulard's solution to determine the recombination efficiency of the specimen surface.

Test conditions are monitored continuously from the start of a HYMETS test. Upon initiation of exposure, the specimen temperature is highly transient, and heat loss by radiation is negligible. After some time the specimen temperature stabilizes, thermal equilibrium conditions are present, and the heat absorption term q_{absorp} in Eq. (7) is negligible. Calculations are made for the thermal equilibrium portion of the test to obtain a value for the recombination efficiency at the test temperature.

Results and Discussion

Figure 2 presents measured weight change data for uncoated and coated NARloy-Z specimens under both static and dynamic oxidation conditions at 920 K. Also included for comparison are data for unalloyed chromium.

These results show that uncoated NARloy-Z specimens experienced a severe loss of weight with oxidation in both static and dynamic environments. Under both conditions the specimens form heavy oxide layers, which are not protective. Upon cooldown, the oxides that form spall from the specimen, exposing bare alloy surface.

The oxidation characteristics of chromium were examined because Cr is a major element in the performance of the Cu-30 vol% Cr coating. The chromium samples experienced a slight increase in weight with exposure to static oxidation conditions but a severe weight loss under dynamic oxidation conditions. XRD data show Cr_2O_3 as the only oxide present on the surface after exposure to either static or dynamic oxidation conditions. These results confirm that the conditions present in the HYMETS are sufficient to accelerate the oxidative evaporation of Cr_2O_3.

The coated specimens experienced little weight change with exposure to either dynamic or static oxidation. There is no distinguishable difference in the weight change history of coated specimens with and without the postcoat oxidation treatment.

Table 2 summarizes the results from XRD analysis of specimen surfaces in the as-coated condition as well as after postcoat oxidation followed by HYMETS exposure. The Cu and Cr exist as heterogeneous components in the as-coated specimen and do not form any compounds. The XRD analysis of the statically oxidized sample indicate that Cr_2O_3 is the primary phase, with only weak signals from CuO identified. This is consistent with previous studies of statically oxidized coated samples[1,2] that have shown that a protective layer of Cr_2O_3 forms underneath a very thin layer of CuO. After 1-h dynamic oxidation at 920 K, strong peaks from CuO and medium peaks from Cr_2O_3 were also detected. After 10-h dynamic oxidation, a strong peak from CuO was still present while the Cr_2O_3 peaks were further reduced in intensity. These results indicate that the Cr_2O_3 layer is still present after 10-h dynamic oxidation but a larger amount of CuO is formed in dynamic oxidation compared to static exposures.

Table 2 XRD results for Cu-30 vol% Cr coating

Exposure conditions[a]	XRD signal strength[b]			
	Cu	Cr	CuO	Cr_2O_3
As coated	vs	s	——	——
Preoxidized	w	w	w	vs
1 h at 920 K	w	w	s	m
10 h at 920 K	w	w	s	vw

[a]Specimens exposed to dynamic oxidation in arc jet (HYMETS facility at NASA Langley Research Center).
[b]Signals: vs, very strong; s, strong; m, medium; w, weak; and vw, very weak.

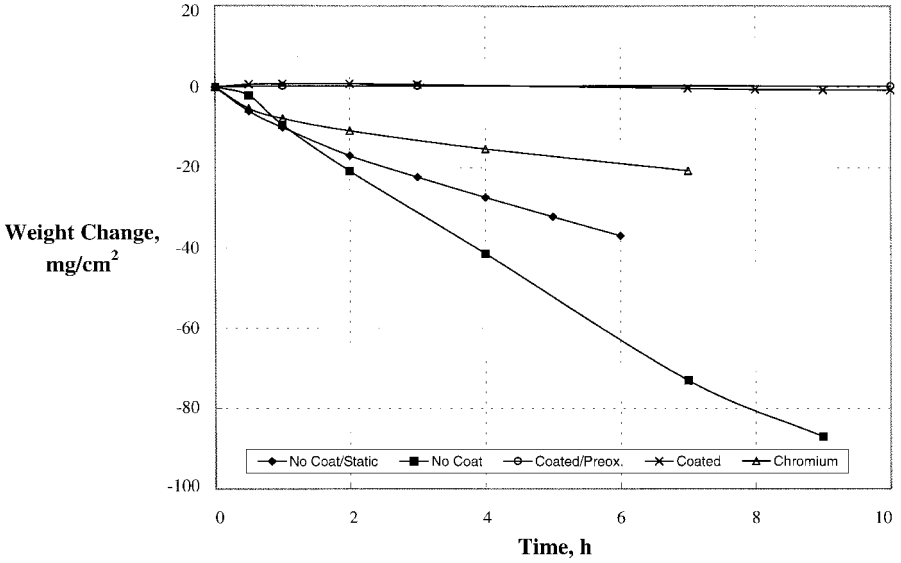

Fig. 2 Oxidation weight change history of NARloy-Z with Cu-30 vol% Cr coating under dynamic conditions.

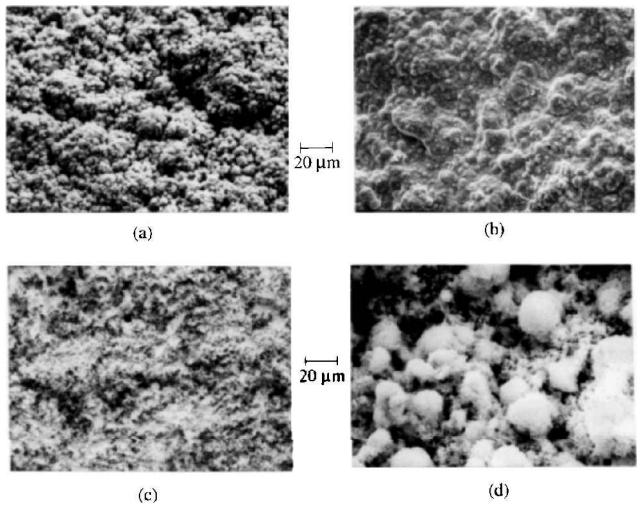

Fig. 3 Scanning electron micrographs of Cu-30 vol% Cr coating surfaces a) as coated, b) after preoxidation, c) after 1-h exposure, and d) after 10-h exposure to dynamic oxidation.

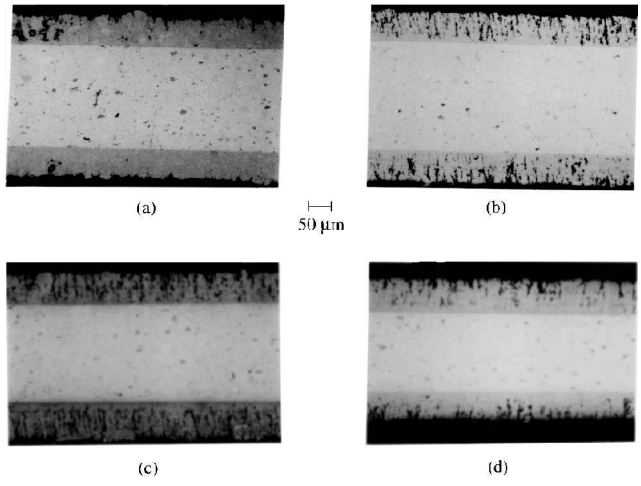

Fig. 4 Photomicrographs of coated NARloy-Z cross sections a) as coated, b) after preoxidation, c) after 1-h exposure, and d) after 10-h exposure to dynamic oxidation.

Scanning electron microscope micrographs of the surface of coated specimens are shown in Fig. 3: specimens as coated and after a preoxidation treatment and after 1- and 10-h exposures at 920 K. The figure shows the surface of specimens with no dynamic oxidation to have a heavily granulated texture. The specimen that has undergone static oxidation was shown by EDS to be covered primarily by Cr_2O_3, with small particles of CuO present. After 1-h exposure, the specimen is covered by a fine oxide, which was shown by EDS to be CuO. After 10-h dynamic oxidation, the surface appearance changes to one covered by spherical oxide, which EDS examination showed to be CuO.

Figure 4 shows light-microscope photomicrographs of cross-sectioned specimens: specimens with and without a postcoat oxidation treatment and specimens with a postcoat oxidation treatment after 1- and 9-h dynamic oxidation exposure at 920 K. The elemental composition of the coating with and without dynamic oxidation exposure was determined by EDS to be within a few percent of the nominal target composition of the coating. The dark regions that appear to be cracks through the coating were determined by EDS to be regions of segregated Cr, with elevated levels of O also present.

Figure 5a shows an SEM micrograph of the top oxide layer of a sample with a postcoat oxidation treatment after 3-h dynamic exposure and Fig. 5b a sample without a postcoat treatment after 10-h dynamic oxidation exposure. EDS examination showed a top layer of CuO on both samples with a continuous layer of Cr_2O_3 beneath

Table 3 Total emittance data for Cu-30 vol% Cr coating

Exposure condition[a]	Total emittance at 920 K
As coated	0.42
Preoxidized	0.66
1 h at 920 K	0.76
3 h at 920 K	0.74
10 h at 920 K	0.68

[a] Specimens exposed to dynamic oxidation in arc jet (HYMETS facility at NASA Langley Research Center).

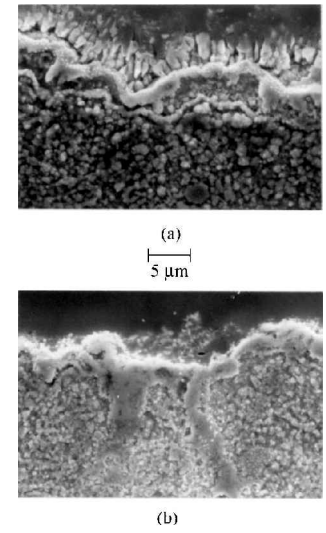

Fig. 5 SEM micrographs of Cu-30 vol% Cr coating cross sections a) preoxidized and then exposed 3 h and b) not preoxidized but exposed 10 h.

it. The sample with the postcoat oxidation treatment had additional layers below this consisting of a layer of mixed Cu and Cr oxides on top of a second continuous layer of Cr_2O_3. This is presumably the remnants of the original oxide before dynamic oxidation.

The analyses outlined here indicate that the low weight gains in dynamic oxidation are due to the formation of a continuous, protective layer of Cr_2O_3. This layer is protected from the environment by a top layer of CuO.

Spectral and total emittance data for coated specimens are presented in Fig. 6 and Table 3, respectively. The emittance of the as-coated specimen is low and typical of unoxidized metal surfaces. The emittance of the coating with the postcoat treatment is significantly higher than for the as-coated specimen. The emittance of coated specimens exposed to dynamic oxidation is even higher than the emittance of either the as-coated or the coated-plus-postcoat-treatment specimens.

The Cu- and Cr-oxides formed during static and dynamic oxidation of coated specimens result in higher spectral and total emittance values compared to data for as-coated specimens, shown in Fig. 6 and Table 3. Under all conditions, the total emittance is lower than the favored minimum emittance of 0.8 for hypersonic vehicles surfaces.[17] The emittance of the coated specimen that received preoxidation treatment is higher than for the as-coated specimen. Exposure to dynamic oxidation further increases the emittance of the coating, indicating that chemical reactions, beyond those that occur under static conditions, occur under dynamic oxidation conditions. The total emittance data in Table 3 show a decrease with time of exposure to dynamic oxidation conditions. The decay in emittance with exposure time is probably related to the decrease in intensity of the oxide phase Cr_2O_3 with time and temperature of exposure under dynamic oxidation conditions.

Figure 7 shows the variations with time of the hot-wall recombination efficiency of coated specimens exposed to dynamic oxidation at 920 K. The recombination efficiency is greater than 0.2 for all specimens evaluated, which is representative of metallic oxide surfaces.

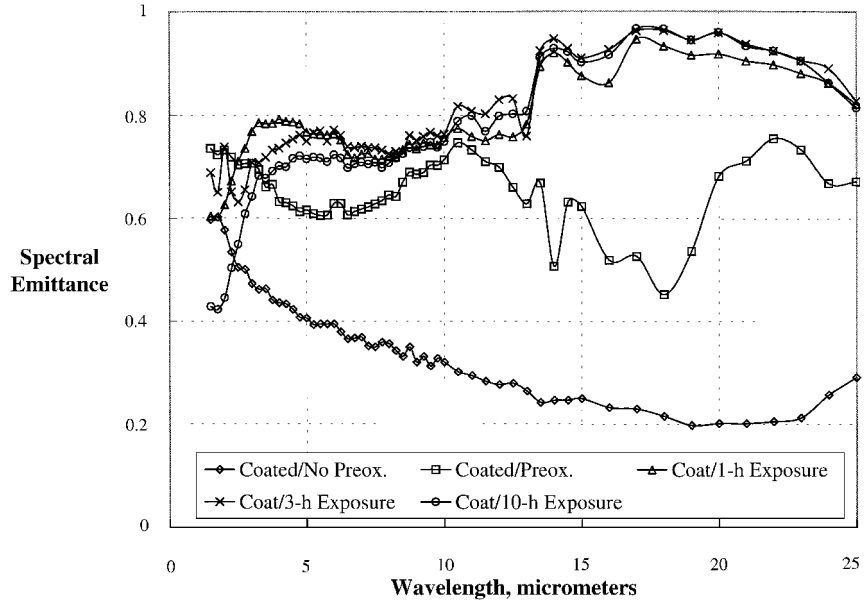

Fig. 6 Spectral emittance of NARloy-Z with Cu-30 vol% Cr coating after dynamic oxidation exposure.

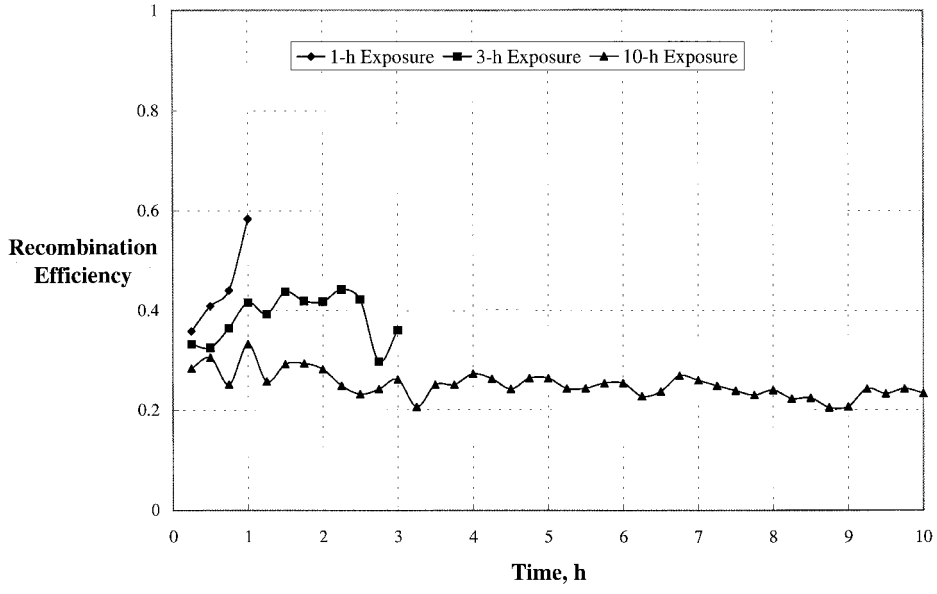

Fig. 7 Hot-wall recombination efficiency of NARloy-Z with Cu-30 vol% Cr coating.

Coatings designed to provide low-recombination efficiency surfaces are typically glasslike and have been shown to provide efficiency levels below 0.02 (Ref. 18).

Concluding Remarks

NARloy-Z specimens coated with a Cu-30 vol% Cr coating were tested under dynamic oxidation conditions at 920 K for up to 10 h. Uncoated specimens were tested for comparison. Uncoated specimens tested under static and dynamic conditions experienced severe weight loss due to the spalling of surface oxides. The coating protects the alloy under dynamic oxidation conditions, with specimens gaining less than 1 mg/cm^2 over a 10-h exposure period.

Examination of coated specimens using SEM, EDS, and XRD showed that Cu and Cr exist in the as-coated specimen as a heterogeneous mixture. On exposure to static or dynamic oxidation conditions, the coating oxidizes to form a mixed oxide containing the phases CuO and Cr_2O_3. Protection of the alloy from oxidation results from a continuous layer of Cr_2O_3 that is partially shielded from the hostile dynamic oxidation/atomic oxygen environment by a layer of CuO.

The spectral emittance of the coating before oxidation is similar to the emittance of metallic surfaces. After oxidation exposure, the emittance is higher and typical of Cu- and Cr-oxides. The hot-wall recombination efficiency of the coating is greater than 0.2, which is representative of oxides of metal.

References

[1]Chiang, K. T., and Yuen, J. L., "Oxidation Studies of Cu-Cr Coated Cu-Nb Microcomposite," *Surface and Coatings Technology*, Vol. 61, Jan. 1993, pp. 20–24.

[2]Chiang, K. T., and Ampaya, J. P., "Oxidation Kinetics of Cu-30vol.%Cr Coating," *Surface and Coatings Technology*, Vol. 78, Feb. 1996, pp. 243–247.

[3]Fryburg, G. C., Kohl, F. J., and Stearns, C. A., "Enhanced Oxidative Vaporization of Cr_2O_3 and Chromium by Oxygen Atoms," *Journal of the Electrochemical Society: Solid-State Science and Technology*, Vol. 121, No. 7, 1974, pp. 952–959.

[4]Tenney, D. R., Young, C. T., and Herring, H. W., "Oxidation Behavior of TD-NiCr in a Dynamic High Temperature Environment," *Metallurgical Transactions*, Vol. 5, May 1974, pp. 1001–1012.

[5]Pinkhosov, E., "Noncrucible Method of and Apparatus for the Vapor Deposition of Material upon a Substrate Using Voltaic Arc in Vacuum," U.S. Patent 4,351,855, Sept. 28, 1982.

[6]Lindfors, P. A., Mularie, W. A., and Wehner, G. K., "Cathodic Arc Deposition Technology," *Surface Coatings Technology*, Vol. 29, Feb. 1986, pp. 275–290.

[7]Randhawa, H., "Cathodic Arc Plasma Deposition Technology," *Thin Solid Films*, Vol. 167, Feb. 1988, pp. 175–185.

[8]Narendrnath, K. R., and Major, D., "Metallization of Plastics Via Low Temperature Arc Vapor Deposition (LTAVD)," *Metallized Plastics 2*, edited by K. L. Mittall, Plenum, New York, 1991, pp. 131–140.

[9]Mann, D., Fessmann, J., Kampschulte, G., and Hopkins, M., "Adherent Metallization of Plastic Composites," *Surface and Coatings Technology*, Vol. 49, Jan. 1991, pp. 168–173.

[10]Schaefer, J. W., Tong, H., Clark, K. J., Suchsland, K. E., and Neuner, G. J., "Analytic and Experimental Evaluation of Flowing Air Test Conditions for Selected Metallics in a Shuttle TPS Application," NASA CR-2531, Aug. 1975.

[11]Clark, R. K., Cunnington, G. R., and Robinson, J. C., "Vapor-Deposited Emittance-Catalysis Coatings for Superalloys in Heat-Shield Applications," *Journal of Thermophysics and Heat Transfer*, Vol. 1, Jan. 1987, pp. 28–34.

[12]Dunkle, R. V., Edwards, D. K., Gier, J. T., Nelson, K. E., and Roddick, R. D., "Heated Cavity Reflectometer for Angular Reflectance Measurements," *Progress in International Research on Thermodynamic and Transport Properties*, edited by J. F. Masi and D. H. Tsai, Academic, New York, 1962, pp. 541–562.

[13]Touloukian, Y. S., and Dewitt, D. P. (eds.), *Thermal Radiative Properties—Nonmetallic Solids*, Vol. 8, Thermophysical Properties of Matter, IFI/Plenum, New York, 1972, p. 18a.

[14]Cunnington, G. R., Funai, A. I., and Cassady, P. E., "Development of Techniques and Associated Instrumentation for High Temperature Emissivity Measurements," NASA CR-124423, June 1973.

[15]Goulard, R., "On Catalytic Recombination Rates in Hypersonic Stagnation Heat Transfer," *Journal of Jet Propulsion*, Vol. 28, Nov. 1958, pp. 737–745.

[16]Clark, R. K., Cunnington, G. R., and Wiedemann, K. E., "Determination of the Recombination Efficiency of Thermal Control Coatings for Hypersonic Vehicles," *Journal of Spacecraft and Rockets*, Vol. 32, No. 1, 1995, pp. 89–96.

[17]Varisco, A., Bell, P., and Wolter, W., "Design and Fabrication of Metallic Thermal Protection Systems for Aerospace Vehicles," NASA CR-145313, Feb. 1978.

[18]Cunnington, G. R., Clark, R. K., and Robinson, J. C., "Thermal Coatings for Titanium-Aluminum Alloys," NASA TM-107760, April 1993.

T. C. Lin
Associate Editor